2016

Experimental Analysis of Latent Heat Storages integrated into a Liquid Cooling System for the Cooling of Power Electronics

Thomas Bezerra Helbing
Institute of Thermo-Fluid Dynamics, Hamburg University of Technology, Germany, thomas.helbing@tuhh.de

Gerhard Schmitz
Institute of Thermo-Fluid Dynamics, Hamburg University of Technology, Germany, schmitz@tuhh.de

Experimental Analysis of Latent Heat Storages integrated into a Liquid Cooling System for the Cooling of Power Electronics

Thomas BEZERRA HELBING[1*], Gerhard SCHMITZ[2]

[1] Hamburg University of Technology, Institute of Thermo-Fluid Dynamics, Applied Thermodynamics, Hamburg, Germany
Phone +49 (0)40 42878-3267, Fax +49 (0)40 42878-2967, thomas.helbing@tuhh.de

[2] Hamburg University of Technology, Institute of Thermo-Fluid Dynamics, Applied Thermodynamics, Hamburg, Germany
Phone +49 (0)40 42878-3144, Fax +49 (0)40 42878-2967, schmitz@tuhh.de

* Corresponding Author

ABSTRACT

This paper presents experimental results of Thermal Energy Storages (TES) implemented into a liquid cooling system for the cooling of power electronics (PE). The experimental investigations are performed on a test rig at Hamburg University of Technology. The main objective of this study is to find a constellation, in which the weight of the liquid cooling system can be reduced by complying with a maximum temperature. For this purpose tests with a Latent Heat Storage (LHS) and a Sensible Heat Storage (SHS) were realised. The results are compared to a direct cooling of power electronics. Finally the weight reduction potential is estimated.

1. INTRODUCTION

The progressive electrification in the automotive and aircraft industry results in increasing power densities and heat losses of power electronics. Due to higher power densities air cooling systems are substituted by more effective but in many cases heavier liquid cooling systems. Since the weight of cooling systems is a crucial aspect during the design process of vehicles, the dimensions of cooling systems should be only as large as necessary.

Dissipated heat of power electronics often implies short periods of high heat flow rates, so called peaks. Liquid cooling systems are usually designed for the maximum heat flow rate, which results in an oversized system for a wide range of operating points. By compensating those peaks with a buffer storage the liquid cooling system can be downgraded and the weight reduced, whereas a trade-off between the weight reduction potential and the additional weight of the buffer storage is essential.

In previous works at the Institute of Thermo-Fluid Dynamics investigations regarding the inner structure of regularly and irregularly structured LHS were carried out in detail (Lohse and Schmitz (2012) and Lohse (2013)). One focus was the design of frame-structures for non-uniformly heat flux distributions, so called hot-spots.

Moreover, simulations in the object-oriented language Modelica were performed during the LuFo IV project NELA-EPE (Neuartige Elektronische Luftfahrtsystem Ansätze - Enhanced Power Electronics). The simulation results indicated a potential of weight reduction. By this time the models weren't validated with experimental data. In order to validate the models and to verify the weight reduction potential, a test rig was built. The first experimental results are presented and discussed in this paper. Furthermore, a weight estimation of the main components of the cooling system is presented.

2. COMPOSITE LATENT HEAT STORAGE AS BUFFER STORAGE

A buffer storage absorbs thermal energy during a peak and releases it after the peak. Basically both main types of TES can be used as buffer storage, LHS and SHS. However, the SHS absorbs the thermal energy by continuously increasing temperature, while the LHS is able to absorb a part of the thermal energy as melting enthalpy, which results in smaller temperature increases. Therefore, the focus in this study is put on the LHS.

LHSs are passive cooling systems based on Phase Change Materials (PCMs), which have the ability to store a high amount of thermal energy during the melting process. Common PCMs in the considered temperature region are paraffins and salt hydrates. The most important material properties when selecting a PCM are melting temperature, latent heat and density. Especially the melting temperature has to be chosen properly in order to ensure the melting of PCMs exclusively during the peak loads (Lohse (2013)).

The low thermal conductivity of most PCMs and in consequence the poor distribution of thermal energy into the PCM can be compensated by using Composite Latent Heat Storages (CLHSs). A CLHS improves the distribution of the thermal energy by a frame-structure of a material with high thermal conductivity, e.g. aluminium, which is filled with PCM. The design of such a frame-structure is a challenge and depends highly on the operating and boundary conditions (Lohse (2013)).

In order to keep the geometry as simple as possible a frame-structure for the CLHS based on regular distributed straight fins is used. A regular distributed structure is a good choice for homogeneous heat sources. It also simplifies modelling and simulation of such a storage in Modelica language, which is one of the objectives in this investigation. However, modelling and simulation of the CLHS or an entire cooling system is not part of this paper.

One important sizing parameter of the cooling system is the mass flow rate, having a direct influence on the junction temperature, which is the highest temperature of a semiconductor. The junction is the interface between the two types of semiconductor materials (e.g. n-type silicon and p-type silicon).

The basic idea of using the CLHS as a buffer storage in this study is to reduce the required mass flow rate by keeping the junction temperature at same level. Alternatively, the mass flow rate can be kept constant in order to reduce the junction temperature. The functionality of the CLHS depends on the positioning of the CLHS, which will be described in the following.

2.1 Positioning

Figure 1 shows the three positioning, which can be implemented within the test rig. Also, the finned frame-structure of the CLHS with the PCM inside can be seen. The fins are arranged orthogonally to the flow direction of the fluid.

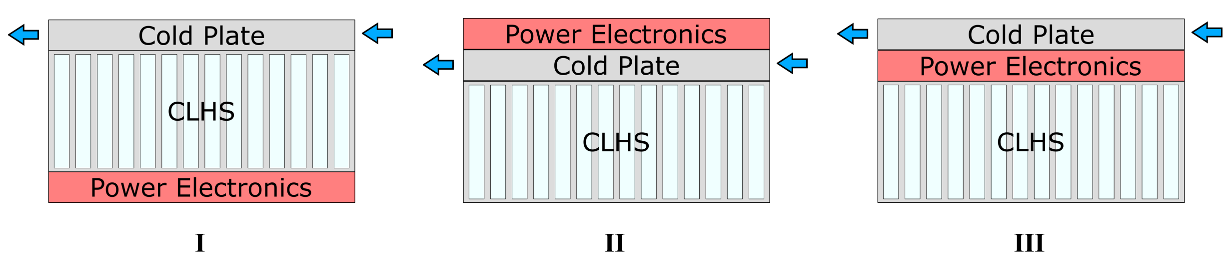

Figure 1: Positioning of the main components.

At the first positioning (I) the CLHS is between cold plate and power electronics. The main advantage of having the CLHS in the middle is the thermodynamical decoupling of power electronics and cold plate, which results in an improved buffering effect. Moreover, the proximity to the power electronics ensures high temperature gradients, which are crucial for an effective melting and solidification of the PCM. However, due to a higher thermal resistance on the thermal path in this configuration the junction temperature is expected to be higher compared to a direct cooling without CLHS. Therefore, implementing a CLHS in this position would at no time result in lower mass flow rates and in consequence in a downgrade of the system.

In the second positioning (II) set-up the cold plate is positioned between the CLHS and the power electronics module. This positioning results in lower mass flow rates. However, the main disadvantage is the low temperature gradient on the cooling surface of the opposite side of the cold plate, since the CLHS has no direct contact to the power electronics module. The effect of this disadvantage can be reduced by integrating the CLHS within the cold plate. Such an integrated CLHS cold plate will be part of future analysis.

Positioning III consists of power electronics with cooling surfaces on both sides. Double-sided cooling of power electronics modules is not only component of research, but also in some cases ready for the market (Kang (2012)). Most of those modules were designed for the automotive industry. This positioning combines the advantage of the proximity of the CLHS to the power electronics module without having the disadvantage of higher thermal resistance. Adding a CLHS in this set-up results always in lower mass flow rates.

All three arrangements are tested and compared with a direct cooling. The most promising is used for the main tests.

3. TEST RIG

In order to validate Modelica models and to perform additional analysis a test rig is built at Hamburg University of Technology. The set-up is described in the following.

3.1 Set-up

The test rig is an one-phase liquid cooling system with a pump, a heat exchanger (HX), a tank, a cold plate (CP) and a power electronics dummy (PE). A dummy is used instead of a real power electronics, since the measurement of the heat loss of cartridge heaters is more accurate. Furthermore, power electronics require additional components for high currents and voltages.

Propylene glycol water (PGW) in a mixture of 60/40 is used as fluid, which is one of the possibly in future implemented cooling fluids for the cooling of power electronics in aircraft. The pump (*Speck NPY-2251-MK*) is able to provide a mass flow rate range of $40\,\mathrm{kg/h}$ to $1200\,\mathrm{kg/h}$.

The test rig schematic is shown in Figure 2 and a photo of the test rig in Figure 3. The pump transports the fluid from the tank to the heat exchanger, where the fluid is cooled down to a specified temperature using a thermostat (*Lauda K6 KP, DLK 40*) . All tests were carried out by an inlet temperature of $20\,^{\circ}\mathrm{C}$ in order to reduce heat losses to ambient. The tempered fluid passes the mass flow sensor and enters a rectangular straight inlet section with a length of 30 hydraulic diameters in order to ensure a fully developed velocity profile. The fully developed flow enters the cold plate, which is a custom-made laser sintered cold plate with staggered pin-fins. The power electronics dummy and the CLHS are pressed on the cold plate by two plates. Thermal interface material with a thermal conductivity of $10\,\mathrm{W/(m\,K)}$ is used between the contact surfaces to reduce the thermal resistance. A torque handle ensures identical contact pressure in all tests.

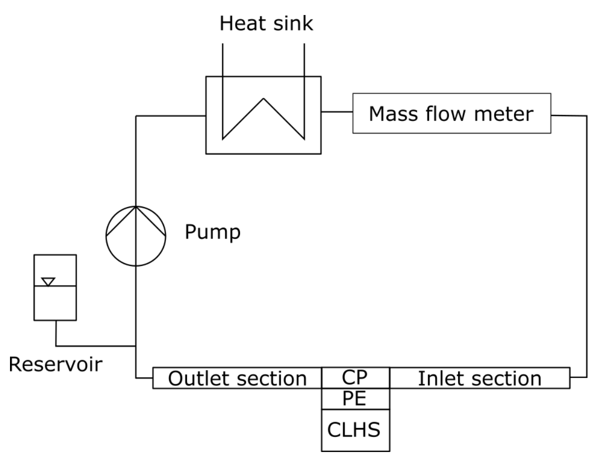

Figure 2: Test rig schematic.

The photo on the right in Figure 3 shows the CLHS. The aluminium fins and the PCM between the fins can be identified. In order to observe the melting process, a plate made of polycarbonate is mounted in front of the CLHS. Behind the

CLHS is a second plate with an air chamber and a silicon membrane to compensate the volume increase during the melting. The weight of the entire CLHS including the polycarbonate plates is 382 g.

The power electronics dummy is a aluminium block with two cartridge heaters, which are able to produce 500 W of maximum waste heat in total, resulting in a maximum heat flux density of 20.8 W/cm^2.

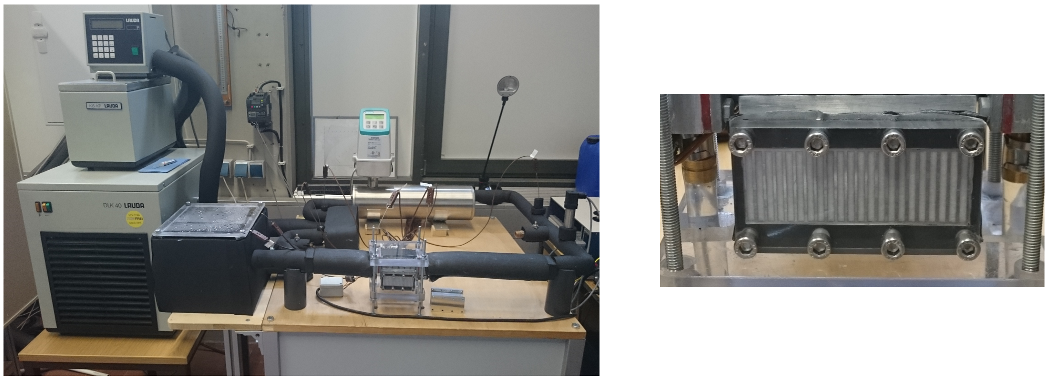

Figure 3: Photos of the test rig and the CLHS.

In the cold plate the waste heat is transferred to the fluid. The pin-fins inside of the cold plates enhances the heat transfer rate, which leads to a good cooling performance.

In this study the maximum allowed junction temperature of the power electronics is set to 65 °C, which is lower than usually allowed temperatures of 80 °C to 90 °C. The reason lies in the high cooling performance of the test rig. In future analysis a higher heat flow rate will be used. Nonetheless, due to simulation results a lower maximum temperature does not effect the results.

3.2 Measurement Equipment

The monitoring is performed by a *National Instruments data acquisition* (DAQ) system including *LabVIEW 2013* for data processing. The temperature measurement is provided by 17 calibrated thermocouples of type T with activated cold junction compensation. Pressure is measured behind the pump and before entering the cold plate by pressure transducers. Also, the pressure loss of the cold plate is measured by a differential pressure sensor.

Optical evaluation is done by a monochrome camera with a resolution of 1920 x 1080 (*Basler acA1920-25um*).

3.3 Material properties of the CLHS

The material properties of the aluminium and PCM used in the CLHS are listed in Table 1. The aluminium alloy is *ENAW 2007*. The paraffin wax *PARAFOL 22-95*® produced by *Sasol Olefins and Surfactants GmbH* is used as PCM (Sasol North America (2016)). Compared to the thermal conductivity the poor heat distribution performance of the *PARAFOL 22-95*® is clear. Otherwise, the wax has the advantage of a significant lower density and higher specific heat capacity.

Table 1: Material properties of aluminum and *PARAFOL 22-95*® (Sasol North America (2016)).

Property	*ENAW 2007*	*PARAFOL 22-95*®
Density ρ in kg/m^3	2850	777
Specific heat capacity c in J/(kg K)	900	3300
Thermal conductivity k in W/(m K)	160	0.162
Melting temperature in °C	-	41.6
Latent heat in kJ/kg	-	250

3.4 Test program

In this study two different heat load profiles of the power electronics are investigated. The first profile has a base load of nearly 95 W and a single peak load of 380 W. Duration and maximum load are defined in respect to the size of the CLHS to ensure an complete melting of the PCM and a maximum temperature of the junction, which is in this case the temperature in the center of the dummy block.

Base load and peak load of the second profile is the same as in the first one. However, the second case has in addition a second peak load, which starts before the PCM is completely solid.

Four tests are realised with the single peak heat load profile. Three tests are performed with a mass flow rate of 40 kg/h and one test with an adapted mass flow rate ($\dot{m}_{\text{adapted}}$). This test is carried out to define the potential of mass flow rate reduction by increasing the temperature continuously till the maximum temperature during the peak is the same as in the test case with CLHS (see Figure 9).

An overview of the tests is shown in Table 2. At the beginning tests with $\dot{m}$ = 40 kg/h are performed: direct cooling without any buffer storage, cooling with an aluminium block as SHS and cooling with a CLHS. The CLHS and SHS storages have identical volumes. The weight of the SHS is 461 g.

Table 2: Test program of single peak profile.

	40 kg/h	$\dot{m}_{\text{adapted}}$
direct	x	x
SHS	x	
CLHS	x	

4. EXPERIMENTAL RESULTS

First, the results of the comparison of the positioning are presented. Based on those results one positioning has been chosen. Afterwards, the test results in order to reduce the weight are presented.

4.1 Comparison of positioning I-III

For the comparison of the positioning (Section 2.1) a heat load profile with one peak has been used. In Figure 4 the junction temperatures of the direct cooling and the tests with positioning I-III are shown. The results are only valid for this type of application and geometry.

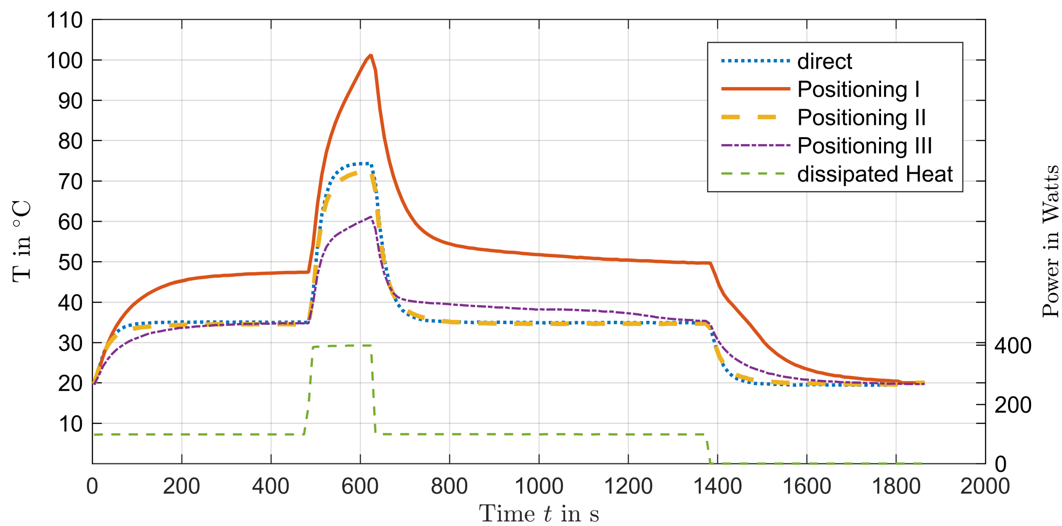

Figure 4: Junction temperature and dissipated heat for the comparison of the positioning ($\dot{m}$ = 40 kg/h).

The blue, dotted line is the junction temperature of the direct cooling and the red, solid line is the junction temperature of the CLHS between PE and CP. The high thermal resistance of the CLHS in positioning I leads to a significant higher temperature of the junction all the time. On the one hand a high amount of thermal energy is stored in the storage, while the amount of thermal energy, which is transported by the fluid, is reduced. On the other hand the main sizing parameter is the maximum junction temperature, which is higher compared to the direct cooling. The good buffering does not result in lower mass flow rates and in consequence in less weight of the cooling system. This positioning has not been used due to those physical constraints.

In positioning II (CP between CLHS and PE) is no direct contact between the CLHS with the PE. The temperature of the CLHS is lower and the PCM remains solid. In this positioning the CLHS has only a small effect on the cooling system, which results in similar curves of the junction temperature compared to the direct cooling.

The yellow, dashed line is the junction temperature of the PE between CP and CLHS. It has the lowest temperature during the peak. This positioning is qualified for a downsizing of the liquid cooling system and has been used for the following tests.

4.2 Weight reduction tests

The results of the tests with one peak are shown in Figure 5. The dashed, purple line is the dissipated heat of the cartridge heaters inside the dummy block. The cartridge heaters are activated from $t = 0$ s to $t = 1380$ s with a base load of about 95 W and a peak load of 380 W. The peak starts at $t = 420$ s and finishes at $t = 630$ s.

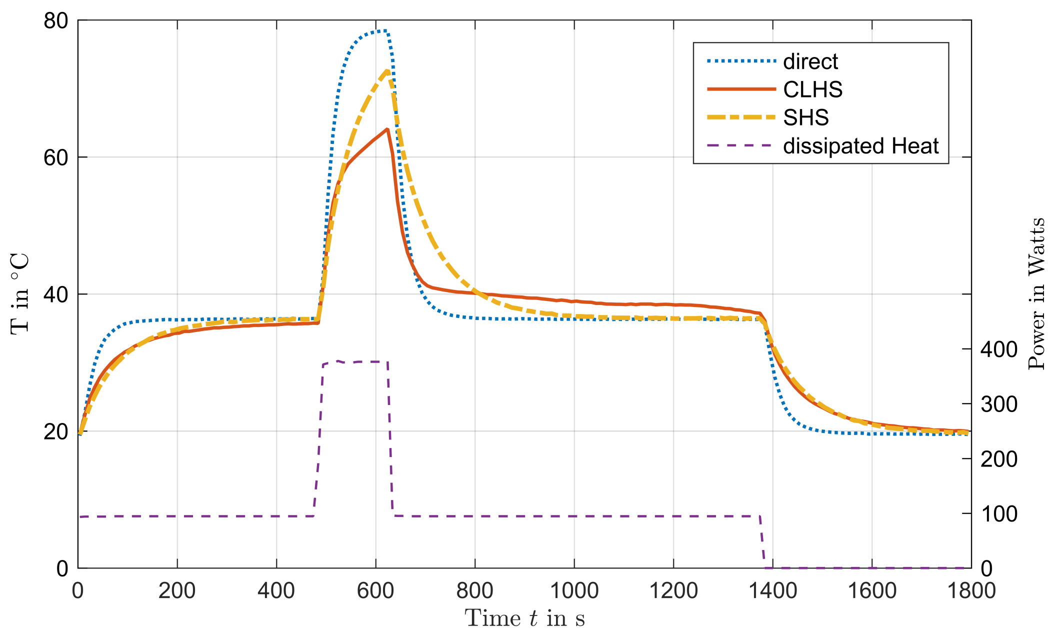

Figure 5: Junction temperature and dissipated heat for the three test cases by a mass flow rate of $\dot{m} = 40\,\mathrm{kg/h}$.

The blue, dotted line shows the junction temperature of the test with direct mounted PE without a buffer storage. The yellow, dashed-dotted line shows the junction temperature of the test with SHS and the red, solid line with CLHS as buffer storage.

After $t = 420$ s the temperatures in all tests are stationary at 36 °C, which is below the melting temperature of the PCM. During the peak the temperature of the direct cooling rises to about 79 °C. The SHS can reduce the temperature by 6 K. The test with CLHS has the lowest temperature during the peak (64 °C). As expected, the test with CLHS is the only one complying with the maximum temperature of 65 °C.

By rising during the peak the temperature curve of the SHS crosses the curve of the CLHS. The SHS has a lower temperature for some seconds. This can be reduced to the high heat conduction of the aluminium in the SHS. At the beginning the heat can be distributed better than in the CLHS, which is the reason why SHSs are good for very short peaks. For long peaks CLHSs are advantageous.

After the peak, the components are cooled down and the CLHS is regenerated. The solidification of the PCM leads to a higher temperature of the PE. However, the temperature is only 4 K higher compared to the direct cooling. Due to the additional thermal capacity for both tests with buffer storages a higher thermal inertia can be observed.

The optical observation of the test with CLHS is shown in Figure 6. Black is solid and white liquid. The PCM starts to melt from top to bottom. The melting starts only during the peak, since the temperature during the base load is below the melting temperature. The PCM starts to melt at the wall and with time the melting region grows to the center of the PCM chamber. After 650 s the entire PCM is liquid.

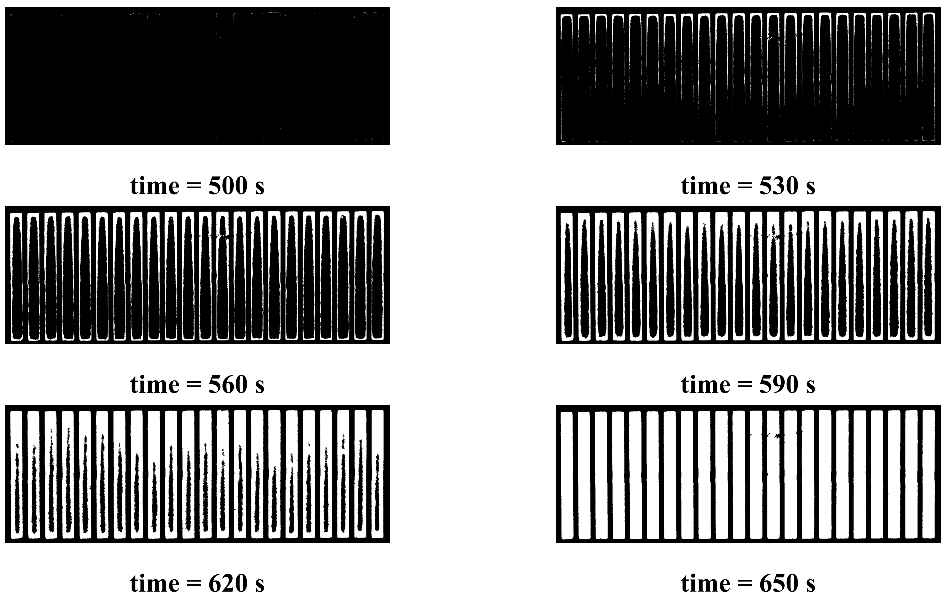

Figure 6: Optical evaluation of the phase change process.

The optical observation is used to determine the liquid fraction over time, which is important for the validation of models. A *MATLAB*® script evaluates for each time step (1 s) the white, liquid area relative to the total PCM area. The result of this evaluation is shown in Figure 7.

As observed in Figure 6, the phase change starts at 500 s with a liquid fraction of 0 and has a liquid fraction of 1 at 650 s. After the peak the components are cooled down. The solidification process is completed after 1130 s, which is 3.2 times longer than the melting process.

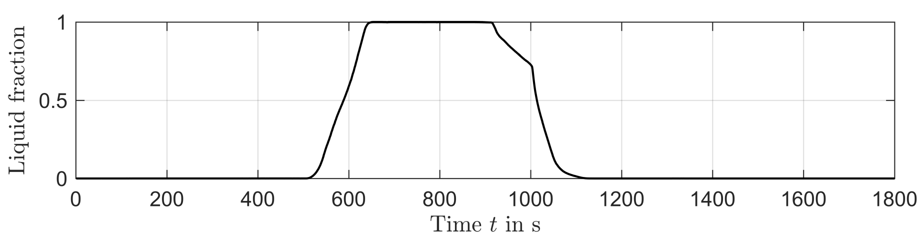

Figure 7: Liquid fraction.

At 1000 s the curve has a buckling, which can be explained by the unequal cooling of the CLHS. While the heat distribution of the cartridge heaters is even, the cooling depends on the fluid temperature, which is the lowest at the entry. Near the entry the PCM starts to solidify early. At 1000 s the remaining PCM starts to solidify resulting in an accelerating decrease of the liquid fraction curve.

Due to the limited cooling performance the solidification process is about 3.2 times longer than the melting process, which is why the solidification process has to be considered when designing the cooling system.

Figure 8 shows the temperature behaviour of the junction for two consecutive peaks, where the solidification after the first peak is not finalized. The temperature during the second peak is higher and has a negative effect on the weight reduction potential.

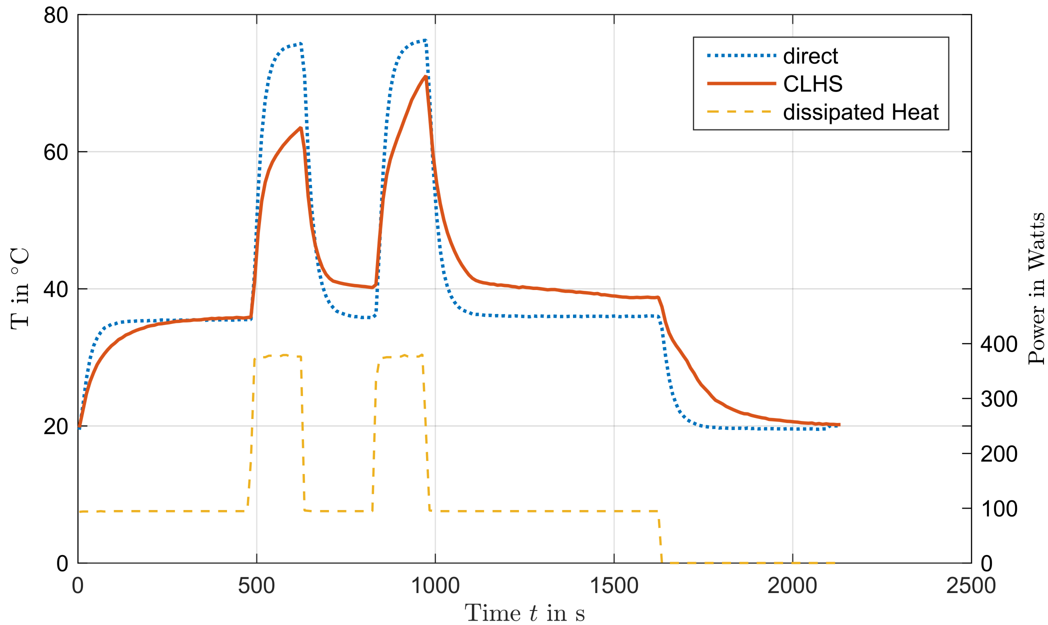

Figure 8: Junction temperature.

In order to find out the reduction potential of the mass flow rate, the mass flow rate is increased in the last test till the same temperature as in the test with CLHS is reached. Figure 9 shows the junction temperature of the test with direct cooling by 40 kg/h and 100 kg/h and the test with CLHS. A cooling system without CLHS would need a 2.5 times higher mass flow rate to keep the maximum allowed temperature conditions.

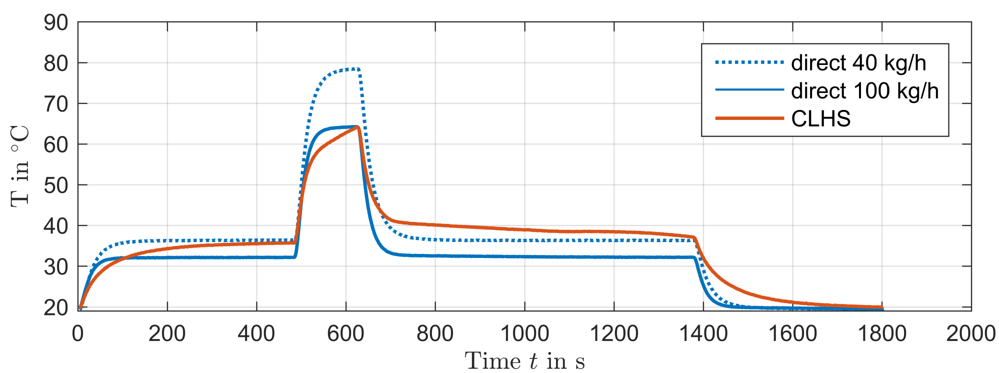

Figure 9: Junction temperature.

5. WEIGHT REDUCTION

The main objective of implementing a CLHS as buffer storage is to reduce the weight of the cooling system. In the following part a simple weight estimation is performed to gain a first impression of the weight reduction potential.

In standard liquid cooling systems a large number of components are installed. In this study two of these components with the most promising potential of weight reduction are picked out, the pump and the pipes with fluid inside.

The pump weight depending on the maximum mass flow rate is shown in Figure 10. Several Speck pumps and Linn pumps of the same type with nearly the same pumping height are marked in the diagram. The fitted curve allows a rough predication of the coherence between weight and volume flow rate for such a pump type. The volume flow rate is converted by a fixed density of the fluid of 1040 kg/m^3 to a mass flow rate.

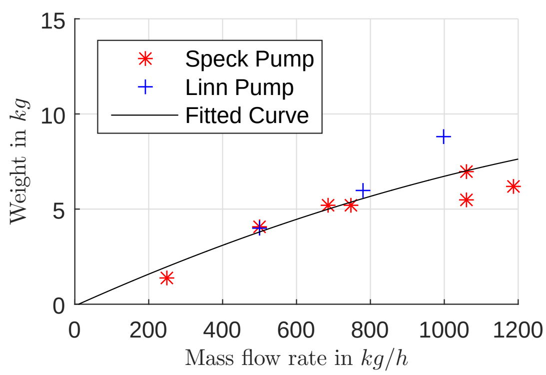

Figure 10: Pump weight estimation

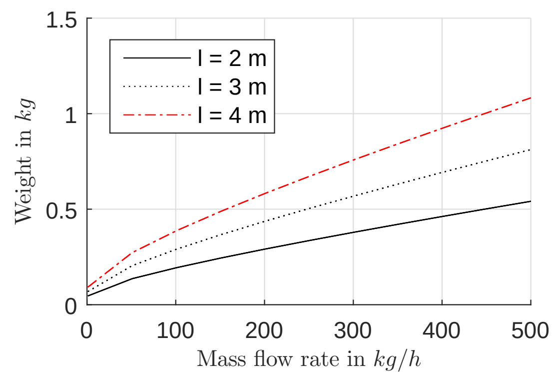

Figure 11: Pipe weight estimation for $v = 1\,\mathrm{m/s}$**.**

The pipe and fluid weight can be calculated by defining some fixed boundary conditions. A fixed velocity of $v = 1\,\mathrm{m/s}$ is assumed for this calculation. The inner radius of the pipe is calculated based on the continuity equation:

$$\dot{m} = v\,\rho\,A = v\,\rho\,\pi\,r^2. \tag{1}$$

By defining a wall thickness of the pipe of $s = 2\,\mathrm{mm}$ the volume and in consequence the mass of the pipe wall and fluid inside of the pipe can be calculated for different pipe lengths. Some exemplary curves are shown in Figure 11.

Due to the results of the tests the mass flow rate for each power electronics module can be reduced from 100 kg/h to 40 kg/h. Assuming a system in aircraft of five power electronics modules with cold plates in parallel the mass flow rate, which has to be provided by the pump, could be reduced from 500 kg/h to 200 kg/h. Regarding the estimations in Figure 10 and Figure 11, the weight of the pump could be reduced from about 3.8 kg to 1.6 kg and in respect to the pipe from about 0.8 kg to 0.44 kg for an overall pipe length of 3 m. This leads to a total weight reduction for each power electronics module of 512 g, which is 34 % higher than the weight of the CLHS (382 g).

This estimation gives a first impression of the weight's savings potential. For real systems a higher weight reduction is expected, since other downgradable system components are missing in the calculation. Also, the weight of the CLHS is higher because of the polycarbonate plates and screws, which are not necessary in a real system.

6. CONCLUSION AND OUTLOOK

This paper presented the results of experiments carried out at a test rig, in order to investigate the benefits on the weight by implementing buffer storages in liquid cooling systems for the cooling of power electronics.

A latent heat storage with inner frame-structure (CLHS) has been used as buffer storage. Different tests with a direct mounted power electronic dummy, a Sensible Heat Storage and a Composite Latent Heat Storage has been carried out.

Regarding the temperature and weight the Sensible Heat Storage performs worse than the CLHS. The CLHS was able to reduce the temperature by 15 K compared to the direct cooling, which results in a reduction of the mass flow rate from 100 kg/h to 40 kg/h and in consequence in a weight reduction of 512 g per power electronics module. Though the additional weight of the CLHS, a weight of 130 g for each power electronics module could be saved by using a smaller pump and pipes.

Since this is a conservative estimation, higher savings are expected in future. A parameter study is planned, in order to identify the coherence of different parameters, e.g. the ratio of the peak load to base load related to the saved mass. Those functions can be helpful for the design of CLHS in future. Furthermore, integrated cold plates with CLHS will be tested.

NOMENCLATURE

ρ	Density	(kg/m^3)
A	Area	(m^2)
B	Liquid fraction	(-)
c	Specific heat capacity	(J/(kg K))
k	Thermal conductivity	(W/(m K))
l	Length	(m)
$\dot{m}$	Mass flow rate	(kg/s)
r	Radius	(m)
s	Wall thickness	(m)
t	Time	(s)
v	Velocity	(m/s)

CLHS	Composite Latent Heat Storage
CP	Cold Plate
DAQ	Data Acquisition System
HX	Heat Exchanger
LHS	Latent Heat Storage
PCM	Phase Change Material
PE	Power Electronics
PGW	Propylene Glycol Water
SHS	Sensible Heat Storage
TES	Thermal Energy Storage

REFERENCES

Kang, S. S. (2012). Advanced cooling for power electronics. In *Integrated Power Electronics Systems (CIPS), 2012 7th International Conference on Integrated Power Electronics Systems (CIPS)*.

Lohse, E. (2013). *Design of Regulary Structured Composite Latent Heat Storages for Thermal Management Applications*. PhD thesis, Hamburg University of Technology.

Lohse, E. and Schmitz, G. (2012). Performance Assessment of Regularly Structured Composite Latent Heat Storages for Temporary Cooling of Electronic Components. *International Journal of Refrigeration*, 35:1145–1155. Issue 4, Elsevier, London.

Sasol North America (2016). Parafol® single cut paraffins – technical bulletin. Technical report, Sasol Germany GmbH. http://www.sasolnorthamerica.com/products/phase-change-materials.